BIOMEDICAL IMAGING BY FLUORESCENT X-RAY MICRO-COMPUTED TOMOGRAPHY

Tohoru TAKEDA,[*1] Tutomu ZENIYA,[1,2] Jin WU,[1] THET-THET-LWIN,[1] Quanwen YU,[1,2] Yoshinori TSUCHIYA,[1] Toru YASHIRO,[1] Tetsuya YUASA,[2] Donepudi V. RAO,[1] Kazuyuki HYODO,[3] F. Avraham DILMANIAN,[4] Yuji ITAI,[1] Takao AKATSUKA[2]

1.Institute of Clinical Medicine, University of Tsukuba, Tsukuba-shi, Ibaraki 305-8575, Japan
2.Faculty of Engineering, Yamagata University, Yonezawa-shi, Yamagata 992-8510, Japan
3.Material Structure Science, High Energy Accelerator Research Organization, Tsukuba 305-0801 Japan
4. Medical Department, Brookhaven National Laboratory, Upton, NY 11973, USA

Abstract: Fluorescent x-ray CT (FXCT) with synchrotron radiation is being developed to detect very low concentration of medium elements. This system consists of a silicon monochromator, an x-ray slit, a scanning table, highly purified germanium detector, and an x-ray CCD detector. Monochromatic x rays at 37 keV energy were collimated into a square pencil beam from 0.025 mm to 1.0 mm in size. FXCT clearly imaged endogenous iodine of thyroid and iodine-labeled BMIPP in the myocardium, whereas transmission x-ray CT could not detect iodine. It indicates that FXCT is a highly sensitive imaging modality capable of detecting very low concentration of iodine, and could be applied to image various biomedical objects.

1. INTRODUCTION

Fluorescent x-ray technique used in the planar mode is one of the most sensitive methods for detecting trace elements of medium or large atomic numbers [1]. This method is applied to assess various kinds of excised biomedical objects, such as the Hg intoxication [2], distribution of cisplatin in cancer therapy [3], and the distribution of Cu, Se, and Zn in renal cancer [4]. It can evaluate very low contents in the order of picogram of elements. However, it requires the specimen to be cut into thin slices and to be scanned with a beam perpendicular to its surface.

Transmission x-ray computed tomography (TXCT), which demonstrates the cross-sectional morphological structures of objects, dose not require the preparation of specimens described above. However, it is not sensitive to trace elements, and concentration of such element is in the order of tens of micro-grams per gram, even when monochromatic synchrotron TXCT of high performance with K-edge energy subtraction of the tracer elements is used [5-8]. The FXCT method described here combines the sensitivity of x-ray fluorescence with the cross-sectional capability of CT to detect very low content of elements for biomedical use.

2. DEVELOPMENT OF FLUORESCENT X-RAY TOMOGRAPHY AND COMPUTED TOMOGRAPHY

Micro-tomography with SR was first implemented to detect iron in the head of a bee in 1987 [9]. Fluorescent x-ray tomography with SR allowed to detect about 200 ng iodine in a volume of 4 mm^3 [10, 11], compared to the limit of 5 mg iodine in a volume of 16.3 mm^3 using x-ray tubes [12]. Linear polarization of SR allows marked reduction of Compton scattering overlapped on the excited Kα fluorescent x-ray line and improves minimal detectability of iodine. In the tomographic approach, the detection limit of excited fluorescent x-rays worsens as the requirement for better spatial resolution in the CT image is imposed. However, FXCT system is highly efficient for detecting the excited fluorescent x-rays compared to the tomographic approaches since the FXCT system does not require intense collimation in detection site. As a result, FXCT can reduce the x-ray exposure to the objects. Recent studies with FXCT system enable us an efficient detection of fluorescent x-rays using phantom studies in 1996 [13, 14], and could detect about 60 ng iodine in a volume of 1 mm^3 employing 37-keV monochromatic x-rays, [15]. Extensive theoretical consideration of FXCT was done in 1991 by Hogan [16].

In order to study the biomedical application, FXCT was first applied to depict the cross sectional distribution of iodine within the thyroid gland, in vitro, at the spatial resolution of 1 mm [17, 18] and less than 0.2-mm [19]. In addition, images with about 0.006 mm spatial resolution of phantom [20] and plant [21] was obtained by FXCT. Micro FXCT imaging of the human thyroid gland [22] and rat myocardium labeled by non-radioactive iodine BMIPP [23] were also done (Table1).

Table 1. Development of fluorescent x-ray tomography and computed tomography

year	Tomography	Computed tomography
1987	Boisseau (iron in the head of a bee, SR)	
1989	Cesareo (iodine in phantom, X-ray tube)	
1991		Hogan (Theoretical consideration of FXCT)
1995	Takeda (iodine in phantom, SR)	
1996		Takeda (iodine in phantom, SR)
1997		Yuasa (FXCT reconstruction algorithm)
1998		Rust (iodine imaging in thyroid, SR)
2000		Takeda (iodine labeled BMIPP in rat heart, SR)
2001		Yu (iodine & xenon in large phantom, SR)

(SR: synchrotron radiation)

3. METHODS AND MATERIALS

The experiment was carried out at the bending-magnet beam line *BLNE-5A of the Tristan accumulation ring (6.5 GeV,* 10 - 30 mA) in Tsukuba, Japan.

3.1 FXCT system

It consists of a silicon (111) double crystal monochromator, a pin diode, an x-ray slit system, a scanning table for subject positioning, a fluorescent x-ray detector with its x-ray collimator, and a transmission x-ray detector with its x-ray shutter (Fig.1). The fluorescent x-ray detector was positioned perpendicular to the incident monochromatic x-ray beam to reduce the amount of stray radiation reaching the detector.

3.2 Detection of incident, fluorescent and transmission x ray

The monochromatic x-ray intensity decreased exponentially owing to the decrease of the ring current, so the change of x-ray intensity was measured by Pin diode operated in the current integration mode. Fluorescent x rays, which are emitted isotropically from the subject along the path of the incident x-ray beam, were detected by a highly purity germanium detector with digital gamma-ray spectrometer. The energy resolution was about 700 eV at 30 keV [24, 25]. The transmission x-ray detector was fiber-optically interface x-ray CCD camera cooled by a Peltier thermoelectric cooling (-35°C). This camera had 1240 x 1024 pixels and its pixel size was a 22.5 μm x 22.5 μm. Data was digitized in 16-bit A/D converter.

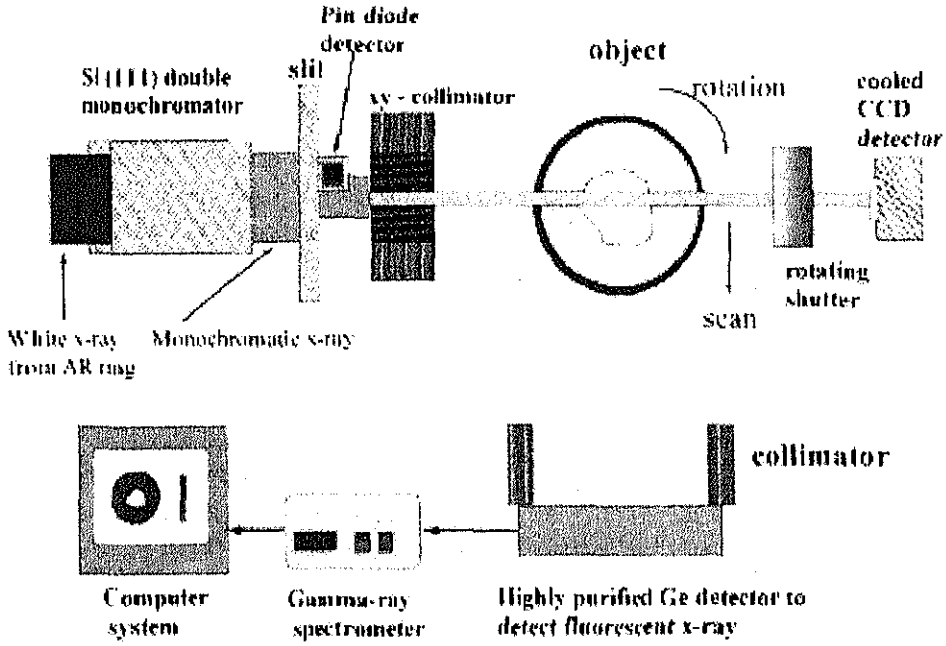

Table 2 Condition of data acquisition

	Sample size (mm)	spatial resolution (mm)	distance HPGe-specimen (mm)	translational step (mm)	rotational step over 180 (degree)	Time (sec)	Doses (Gy)
Thyroid	20	1	200	1	3	5	0.912
	10	0.1	45	0.1	1.2	5	2.564
	2	0.025	20	0.025	1.2	5	2.829
Heart	15	0.3	60	0.3	2.4	5	0.966
	10	0.2	45	0.2	2	5	1.538
	10	0.1	45	0.1	1.5	10	4.103

3.3 System control and image reconstruction

A computer controlled the pulse motor controller. The pulse motor controller controlled the translation-rotation table and rotating x-ray shutter. An automated data-collection procedure was developed using "Labview".

The net counts under the characteristic fluorescent Kα x-ray spectral lines at each projection were used to generate a CT projection. The x-ray fluorescent data were corrected for the attenuation of the incident beam and the emitted fluorescent x-ray, using the attenuation information from the transmission x-ray CT image data. Finally, the FXCT image was reconstructed by an algebraic method including the attenuation process [26].

3.4 Experimental condition of FXCT: X-ray energy selection and the formulation of pencil beam

The white x-ray beam was monochromatized at 37.0 keV and the photon flux rate before the object was 7 x 10^7 photons/mm^2/s at a beam current of 30 mA. The incident monochromatic x ray was collimated into a 1.0 mm x 1.0 mm to a 0.025 mm x 0.025 mm pencil beam (Table 2). Data acquisition time of CCD camera was 0.2-s at each scanning step.

3.5 Object

The objects were a 10-mm-diameter acrylic phantoms with three 3-mm-holes filled with iodine solutions, rat myocardium labeled BMIPP and human thyroid tissues fixed in 10% formalin. Phantom images were obtained to achieve a quantitative estimation for the iodine content of the object. Non-radioactive iodine labeled BMIPP (iodine content of total injection dose: 0.1 mg) which reveals the metabolic state of fatty acid, was injected into living rat heart under the Langendorf procedure. The heart labeled with BMIPP was fixed by formalin. The present experiment was approved by the Medical Committee for the Use of Animals in Research of the University of Tsukuba, and it conformed to the guidelines of the American Physiological Society.

4. RESULTS AND DISCUSSION

4.1 Phantom experiment

In the 3-hole phantom image, the 5μg/ml iodine solution could be visualized at 0.1 x 0.1 mm^2 spatial resolution with 0.1 mm slice thickness by FXCT. Observation of the 5μg/ml iodine solution indicated that the excited iodine content in the measured voxel is about 5 pg (5μg/ml x 1 x 10^{-6} ml). A linear correlation was observed between the iodine concentration and fluorescent x-ray counts in the phantom study (Fig.2). Then, FXCT may be used to detect iodine at low concentration quantitatively.

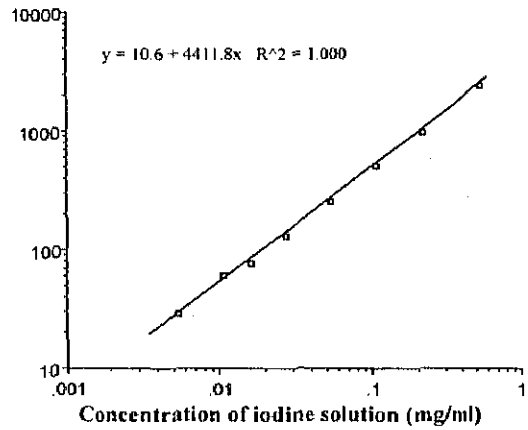

Fig.2 The relationship between fluorescent x-ray counts and iodine concentration

4.2 FXCT image of thyroid specimens

In normal thyroid, the heterogeneous iodine distribution by FXCT caused inhomogeneous distribution of the iodine, vessel structures and connective tissues. Since the transmission x-ray CT cannot distinguish the histopathological structures of soft tissue due to the poor signal to noise ratio, a combined analysis using both FXCT and conventional pathological image is necessary to differentiate various tissues not including iodine such as vessels and connective tissues. In thyroid cancer, cancer lesion was shown as defect because the content of iodine in

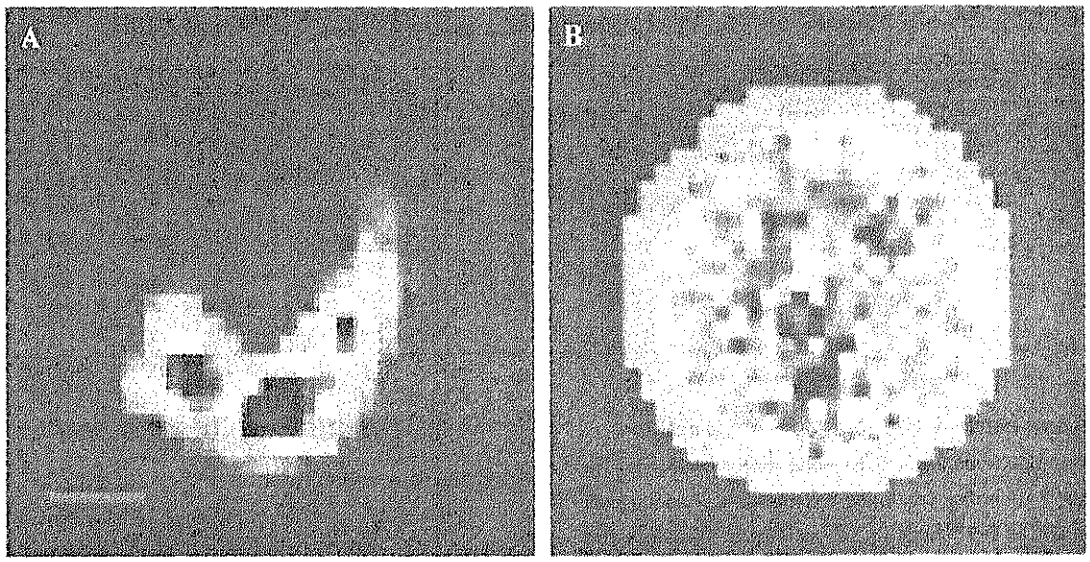

Fig.3 Fluorescent x-ray CT and transmission x-ray CT images of thyroid cancer at 1-mm spatial resolution.
A: Upper defect like area and lower iodine containing area correspond to cancer and normal thyroid respectivel.y.
B: The distribution of iodine cannot be revealed at all by transmission x-rat CT.

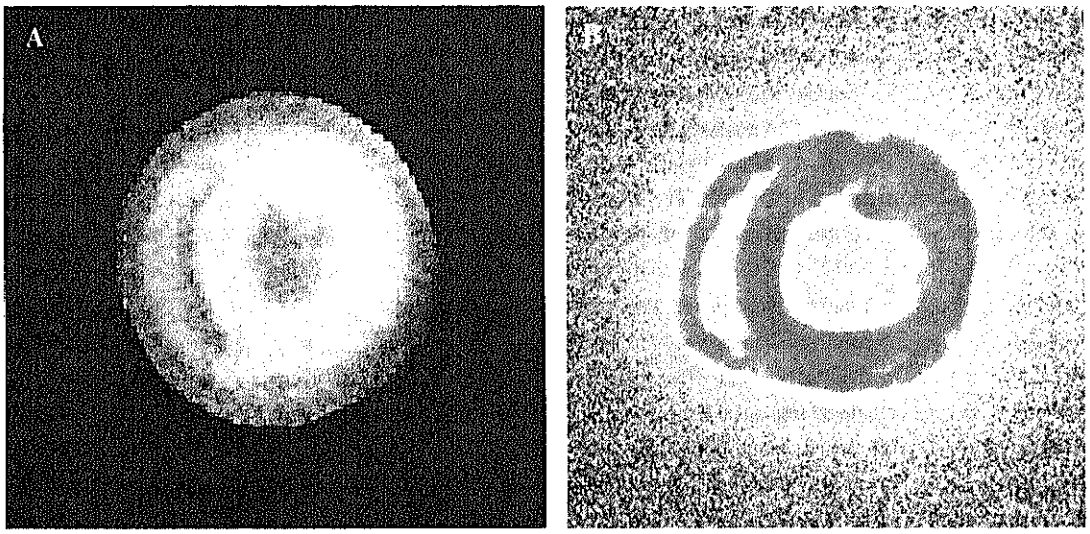

Fig.4 Fluorescent x-ray CT image of rat myocardium labeled by BMIPP.
A FXCT with 0.3mm spatial resolution can reveal homogeneous distribution of BMIPP in normal heart.
B: Autoradiogram with radioactive I-125 BMIPP.
Almost same quality of image resembled to FXCT is observed with a slice thickness of 0.05mm.

cancer was in small amounts comparing to normal thyroid (Fig.3). Quantitative analysis revealed the concentration of iodine within cancer was less than 0.2 mg/g. Effectiveness of ^{131}I therapy might be predicted because the accumulation dose of ^{131}I in thyroid cancer can be estimated by FXCT [27].

4.3 FXCT image of rat myocardium

FXCT image could clearly reveal the distribution of ^{127}I-BMIPP within myocardium both at 0.3 mm spatial resolution and 0.3 mm slice thickness (Fig.4). The content of iodine in myocardium was estimated to be about 0.01 mg/g from the fluorescent Kα counts. Thus, FXCT will be used to evaluate the distribution of labeling elements resembled to the autoradiogram with radio-active agents.

4.4 Present limitations and future plans

In our FXCT system, the obtainable spatial resolution was limited to 25μm owing to the precision of mechanical system. Now a new system is being constructed to obtain a 5μm spatial resolution. Imaging for micrometer spatial resolution requires very long data acquisition time because the scan number of translation and rotation increase significantly. The count-rate capability of HPGe detector with DSPEC

electronics has improved 6-fold as compared to the previous detector system [24]. However, new FXCT system is being designed to acquire image data at 4-times faster than present system; it will use two detectors positioned symmetrically on both sides of the object, and new electronics with much higher count-rate capability. By renewal of Tristan AR ring, the storage current will be 70 mA (present 30 mA) and the life becomes more than 12 hr (present 2 hr).

5. CONCLUSION

The high spatial resolution and high sensitivity of FXCT indicate the potential of this new imaging modality to use various research applications in vitro specimen studies

ACKNOWLEDGEMENT

We would like to thank Mr. Y. Hasegawa for their help with FXCT experiment and Mr. K. Kobayashi for his preparation of experimental apparatus. This research was partially supported by a Grant-in-aid for Scientific Research (#10557084, 12307018 and 13470178) from the Japanese Ministry of Education, Science and Culture, and was performed under the auspices of the National Laboratory for High Energy Physics (Proposal: 99G124, 2001G380).

REFERENCES

1. Iida A, Gohshi Y.: Tracer element analysis by X-ray fluorescent. pp307-348 Handbook on Synchrotron Radiation. Vol 4 1991 edited by Ebashi S, Koch M, Rubenstein E. North-Holland, Elsevier Publisher, Amsterdam.
2. Shimojo N, Homma S, Ohuchi K, Shinyashiki M, Sun GF, Kumagai Y. Mercury dynamics in hair of rats exposed to methylmercury by synchrotron radiation x-ray fluorescence imaging. Life Science 60: 2129-2137, 1997
3. Jonson R, Mattsson S, Unsgaard B.: A method for in vivo analysis of platinum after chemotherapy with cisplatin. Phy. Med. Biol. 33:847-857, 1988
4. Homma S, Sasaki A, Nakai I, Sagai M, Koiso K, Shimojo N. Distribution of copper, selenium, and Zinc in human kidney, tumors by nondestructive synchrotron radiation x-ray fluorescence imaging. J. Trace Elements in Experimental Medicine 6: 163-170, 1993
5. Kazama M, Takeda T, Akiba M, Yuasa T, Hyodo K, Ando M, Akatsuka T, Itai Y. Performance study of monochromatic synchrotron x-ray computed tomography using a linear array detector. Med. Imag. Tech. 15: 615-624, 1997
6. Takeda T, Kazama M, Zeniya T, Yuasa T, Akiba M, Uchida A, Hyodo K, Akatsuka T, Ando M, Itai Y. Development of a monochromatic x-ray computed tomography with synchrotron radiation for functional imaging. Edited by Ando M, Uyama C. Medical Applications of Synchrotron Radiation. pp103-110, Springer-Verlag, Tokyo, 1998
7. Grodzins L. Optimum energies for X-ray transmission tomography of small samples. Application of synchrotron radiation to computed tomography I. Nucl. Instr. Meth. 206: 541-545, 1983
8. Dilmanian FA, Wu XY, Parsons EC, Ren B, Kress J, Button TM, Chapman LD, Coderre JA, Giron F, Greenberg D, Krus DJ, Liang Z, Marcovici S, Petersen MJ, Roque CT, Shleifer M, Slatkin DN, Thomlinson WC, Yamamoto K, Zhong Z. Single- and dual-energy CT with monochromatic synchrotron x-rays. Phys. Med. Biol. 42:371-387, 1997
9. Boisseau P, Grodzins L. Fluorescence tomography using synchrotron radiation. Hyperfine Interactions 33: 283-292, 1987
10. Takeda T, Maeda T, Yuasa T, Akatsuka T, Ito K, Kishi K, Wu J, Kazama M, Hyodo K, Itai Y.: Fluorescent scanning x-ray tomography with synchrotron radiation. Rev. Sci. Instrum. 66 :1471-1473, 1995
11. Takeda T, Maeda T, Yuasa T, Akatsuka T, Ito K, Kishi K, Wu J, Kazama M, Hyodo K, Itai Y.: Fluorescent scanning x-ray tomographic image with monochromatic synchrotron x-ray. Med. Imag. Tech. 14:183-194, 1996
12. Cesareo R., Mascarenhas S.: A new tomographic device based on the detection of fluorescent X-rays. Nucl. Instr. Meth. A 277: 669-672, 1989
13. Takeda T, Akiba M, Yuasa T, Akatsuka T, Kazama M, Hoshino Y, Hyodo K, Dilmanian FA, Akatsuka T, Itai Y.: Fluorescent x-ray computed tomography with synchrotron radiation using fan collimator. SPIE 2708: 685-695, 1996
14. Akiba M, Takeda T, Yuasa T, Uchida A, Hyodo K, Akatsuka T, Itai Y. Fluorescent x-ray computed tomography using synchrotron radiation for imaging nonradioactive tracer materials. Med. Elec. Biol. Eng. 35:303-312, 1997 (Abstract in English)
15. Takeda T, Yuasa T, Hosino A, Akiba M, Uchida A, Kazama M, Hyodo K, Dilmanian FA, Akatsuka T, Itai Y.: Fluorescent x-ray computed tomography to visualize specific materials distribution. SPIE, 3149: 160-172, 1997
16. Hogan JP., Gonsalves RA., Krieger AS. : Fluorescent computer tomography: A model for correction of X-ray absorption. IEEE Transactions on Nuclear Science 38:1721-1727, 1991
17. Rust GF, Weigelt J.: X-ray fluorescent computed tomography with synchrotron radiation. IEEE Trans.Nucl.Sci. 45: 75-88, 1998
18. Takeda T, Yu Q, Yuasa T, Hasegawa Y, Yashiro T, Itai Y.

Human thyroid specimen imaging by fluorescent x-ray computed tomography with synchrotron radiation. SPIE Proceeding 3772: 258-267, 1999

19. Takeda T, Momose A, Yu Q, Yuasa T, Dilmanian FA, Akatsuka T, Itai Y: New types of x-ray computed tomography with synchrotron radiation: fluorescent x-ray CT and phase-contrast x-ray CT with interferometer. Cellular & Molecular Biology 46: 1077-1088, 2000
20. Simionovici AS, Chukalina M, Drakopoulos M, Snigireva I, Snigirev A, Schroer Ch, Lengeler B, Janssens K, Adams F. X-ray fluorescent microtomography: Experiment and reconstruction. SPIE 3772: 304-310, 1999
21. Schroer Ch, Tummler J, Gunzler TF, Lengeler B, Schroder WH, Kuhn AJ, Simionovici AS, Snigirev A, Snigireva I. Fluorescent microtomography: External Mapping of elements inside biological samples. SPIE 4142: 287-296, 2000
22. Takeda T, Yu Q, Yashiro T, Zeniya T, Wu J, Hasegawa Y, Thet-Thet-Lwin, Hyodo K, Yuasa T, Dilmanian FA, Akatsuka T, Itai Y. Iodine imaging in thyroid by fluorescent X-ray CT with 0.05 mm spatial resolution. Nucl. Instr. Meth. A467/468:1318-1321, 2001
23. Takeda T, Matsushita S, Wu J, Yu Q, Thet-Thet-Lwin, Zeniya T, Yuasa T, Hyodo K, Dilmanian FA, Akatsuka T, Itai Y: Fluorescent x-ray CT image of rat heart with non-radioactive iodine labeled BMIPP. Proceeding of IEEE-EMBS Asia-Paciffic Conference on Biomedical Engineering: 276-277, 2000
24. Yu Q, Takeda T, Yuasa T, Hasegawa Y, Akatsuka T, Itai Y. Development of high resolution fluorescent x-ray CT with synchrotron radiation. Med. Imag. Tech. 17: 493-494, 1999
25. Yu Q, Takeda T, Yuasa T, Hasegawa Y, Wu J, Thet-Thet-Lwin, Hyodo K, Dilmanian FA, Itai Y and Akatsuka T. Preliminary experiment of fluorescent X-ray computed tomography to detect dual agents for biological study. J. Synchrotron Rad. 8: 1030-1034, 2001
26. Yuasa T, Akiba M, Takeda T, Kazama M, Hoshino Y, Watanabe Y, Hyodo K, Dilmanian FA, Akatsuka T, Itai Y.: Reconstruction method for fluorescent x-ray computed tomography by least-squares method using singular value decomposition. IEEE trans. Nucl. Sci. 44:54-62, 1997
27. Patton J. A., Sandler M. P., Partain C. L.: Prediction of benignancy of the solitary Cold thyroid nodule by fluorescent scanning. J. Nucl. Med. 26:461-464, 1985